

Lawrence Berkeley National Laboratory

Recent Work

Title

THE RATE-CONTROLLING MECHANISM OF SLIP IN THE INTER-METALLIC COMPOUND AgMg
AT LOW TEMPERATURES

Permalink

<https://escholarship.org/uc/item/35r1p61k>

Authors

Mukherjee, A.K.
Dorn, John E.

Publication Date

1963-08-12

University of California
Ernest O. Lawrence
Radiation Laboratory

THE RATE-CONTROLLING MECHANISM OF SLIP
IN THE INTERMETALLIC COMPOUND
AgMg AT LOW TEMPERATURES

TWO-WEEK LOAN COPY

*This is a Library Circulating Copy
which may be borrowed for two weeks.
For a personal retention copy, call
Tech. Info. Division, Ext. 5545*

DISCLAIMER

This document was prepared as an account of work sponsored by the United States Government. While this document is believed to contain correct information, neither the United States Government nor any agency thereof, nor the Regents of the University of California, nor any of their employees, makes any warranty, express or implied, or assumes any legal responsibility for the accuracy, completeness, or usefulness of any information, apparatus, product, or process disclosed, or represents that its use would not infringe privately owned rights. Reference herein to any specific commercial product, process, or service by its trade name, trademark, manufacturer, or otherwise, does not necessarily constitute or imply its endorsement, recommendation, or favoring by the United States Government or any agency thereof, or the Regents of the University of California. The views and opinions of authors expressed herein do not necessarily state or reflect those of the United States Government or any agency thereof or the Regents of the University of California.

UNIVERSITY OF CALIFORNIA
Lawrence Radiation Laboratory
Berkeley, California

Contract No. W-7405-eng-48

THE RATE-CONTROLLING MECHANISM OF SLIP
IN THE INTERMETALLIC COMPOUND AgMg AT LOW TEMPERATURES

by
A. K. Mukherjee¹ and John E. Dorn²

August 12, 1963

¹ Post Doctoral Research Metallurgist, Inorganic Materials Research Division, Lawrence Radiation Laboratory, University of California, Berkeley.

² Miller Professor of Materials Science 1962-63, Department of Mineral Technology; Research Metallurgist, Inorganic Materials Research Division of the Lawrence Radiation Laboratory, University of California, Berkeley.

ABSTRACT

The effect of strain rate and temperature on the critical resolved shear stress for $(\bar{3}21) [111]$ slip was determined for the CsCl type of intermetallic compound AgMg: The flow stress increased only slightly as the test temperature was first decreased below room temperature, a rapid increase in the flow stress was obtained with yet further decrease in temperature from about 250°K to 4°K . The effect of both the temperature and strain-rate on the flow stress over the low temperature range could be rationalized satisfactorily in terms of the Peierls mechanism when the deformation was controlled by the rate of nucleation of pairs of kinks.

INTRODUCTION

In spite of the well documented interest of metallurgists and engineers concerning the mechanical behaviour of intermediate phases and intermetallic compounds, very little definitive information is available on this important subject. As recently summarized by Westbrook,¹ only limited and modest progress has been made thus far in elucidating the details of the mechanism of plastic deformation for the intermetallic compounds; the available information largely concerns phenomenological descriptions of empirical observations and experimental facts, principally with reference to polycrystalline aggregates.

The present report on the elucidation of the rate-controlling mechanism for slip in the BCC structure of AgMg is part of the comprehensive program of a systematic investigation on the mechanical behaviour of intermetallic compounds.

The intermetallic compound AgMg has a CsCl type of lattice structure² and is completely ordered up to its melting point of 820°C.³ This material was selected for our present investigation because of its simple crystal structure, moderate and congruent melting point, ordered structure persisting up to the melting point, and some solubilities of the constituent elements, which could be expected to help in the growing of single crystal specimens. Whereas previous investigations on the properties of AgMg include hardness,⁴⁻⁶ slip systems,⁷ tensile flow stress of polycrystalline specimens⁸ and electrical resistivity,⁴ the current investigation will be directed principally at elucidating the rate-controlling dislocation mechanism responsible for slip in single crystals at low temperatures. It will be shown that the strain rate depends on the rate of nucleation of pairs of kinks by the Peierls mechanism for plastic deformation.

EXPERIMENTAL TECHNIQUES

Single crystal specimens of the AgMg intermetallic compound were prepared and tested as follows:

1. A master alloy ingot of AgMg was produced by melting and chill casting the high purity Ag (99.995 wt. pct.) and high purity Mg (99.997 wt. pct.) in an induction furnace under a helium atmosphere.

2. Sections of the above mentioned ingot were placed in a graphite mold containing a spherical cavity in which a single crystal sphere of 1 inch diameter was grown under helium by the Bridgeman technique.

3. The operative slip systems were investigated at room temperature on a single crystal of AgMg, from measurements of the angles made by the slip traces on the two surfaces of the specimen, which were at 90° to each other. The investigation confirmed that the AgMg compound undergoes slip primarily in the $(\bar{3}21)$ plane and in the $[111]$ direction, but a small amount of secondary slip was also noticed in the $\{112\}\langle 111 \rangle$ system. No slip was observed in the (110) planes.

4. The single crystal sphere, mentioned earlier, was oriented in a graphite mold containing a cylindrical cavity of $3/8$ " diameter above the spherical receptacle to give the angle $\chi_o = 45^\circ$ between the axis of the cylindrical bar and the normal to the slip plane $(\bar{3}21)$, and the angle $\lambda_o = 45^\circ$ between the slip direction $[111]$ and the axis of the bar. Oriented single crystal bar seeds were produced by melting, under a He atmosphere, a polycrystalline bar in the cylindrical cavity above the oriented spherical seed and by growing an oriented single crystal bar from the seed.

5. Finally, oriented single crystal specimens were grown from these cylindrical seeds.

6. The cylindrical specimens were machined in a High Tension Spark Cutting unit to give a two inch gauge length. The spark machined gauge section was electropolished in a bath containing 200 ml. of H_3PO_4 , 200 ml. of $C_2H_5(OH)$ and 400 ml. of H_2O , using a 5 volt and 60 amp. per sq. inch anode current density. The electropolishing was continued until a 150 micron layer of material was dissolved away in order to ensure that all deformation put into the specimen during spark machining was removed. The specimens were then annealed at $400^\circ C$ for 1/2 hour.

7. The initial orientation χ_o and λ_o of each specimen was determined by the Laue back-reflection technique to within $\pm 1^\circ$.

8. Tension tests conducted below room temperature were carried out by complete immersion of the specimen in different constant temperature baths. Tests at $4^\circ K$ and $23^\circ K$ were carried out in a special cryostat. Tests above room temperature were conducted in a silicone oil bath with an accuracy of control of $\pm 1/2^\circ K$, up to $396^\circ K$.

9. Tension tests were made with an Instron Testing Machine operated at a strain rate of 1.66×10^{-4} per second and 4.16×10^{-6} per second. Stresses were determined to within $\pm 2 \times 10^6$ dynes/cm² and tensile strains were measured to within ± 0.0001 .

EXPERIMENTAL RESULTS AND DISCUSSION

Composition

The composition of the single crystal specimens was chemically analysed for Ag and Mg content. Samples for analysis were taken from two extreme ends of the gauge length in order to ascertain the variation in composition along the gauge length. Table I shows the results of the chemical analysis.

Analysis of specimen tested at	%Mg	<u>Table I</u>	
		Difference between top and bottom %Mg	Difference between top and bottom %Ag
4°K	Top 17.75	0.15	Top 82.11
	Bottom 17.90		Bottom 81.97
77°K	Top 17.75	0.24	Top 82.02
	Bottom 17.99		Bottom 81.91
141°K	Top 17.85	0.07	Top 82.00
	Bottom 17.92		Bottom 82.14
250°K	Top 17.76	0.03	Top 81.99
	Bottom 17.79		Bottom 82.12

The stoichiometric AgMg compound contains 81.6 wt. pct. Ag. It was obvious that during remelting, in order to grow single crystal specimens of AgMg, there had been some loss of Mg with a consequent increase in Ag content. But the average Ag content was still within 0.43 wt. pct. of the stoichiometric composition and the maximum variation of the Ag content from one specimen to another was less than 0.25 wt. pct.

Effect of Temperature and Strain-Rate on Flow Stress

In order to obtain a reproducible data from each crystal, each specimen was prestrained at 273°K and 1.66×10^{-4} per sec. strain-rate to a stress level

approximately 1% above the yield stress, so as to give a standard level of dislocation density. Figure 1 is a representation of the experimentally determined yield stress versus temperature diagram for single crystals of AgMg. The applied shear stress that is required to cause plastic flow is given by

$$\tau = \tau^* + \tau_A \tag{1}$$

where τ^* is the stress required to aid the thermal activation of the rate controlling mechanism and therefore decreases precipitously as T increases, and τ_A is the stress necessary to overcome such athermal mechanisms as long-range back stresses, short-range order stresses, etc., and therefore decreases only modestly as the temperature decreases, usually parallel to the shear modulus of elasticity.

In our present discussion we are primarily interested in the effect of temperature on the thermal component τ^* and would like to separate it from others. This could be done by subtracting the stress at a given temperature T from that at some standard temperature, eg., $T_{273^{\circ}\text{K}}$, as shown in Eqn. 2.

$$\tau^* = \tau_T - \tau_{273} \frac{G_T}{G_{273}} \tag{2}$$

where τ_T is the total resolved shear stress for flow at temperature $T^{\circ}\text{K}$ and G_T is the shear modulus of elasticity at temperature $T^{\circ}\text{K}$. The quantity $\tau_{273} \frac{G_T}{G_{273}}$ is then the total back stresses, corrected for change in shear modulus with temperature. The values of $\frac{G_T}{G_{273}}$ were calculated from Fig. 2, which shows the variation of G with temperature, as taken from the data of Chang.⁹

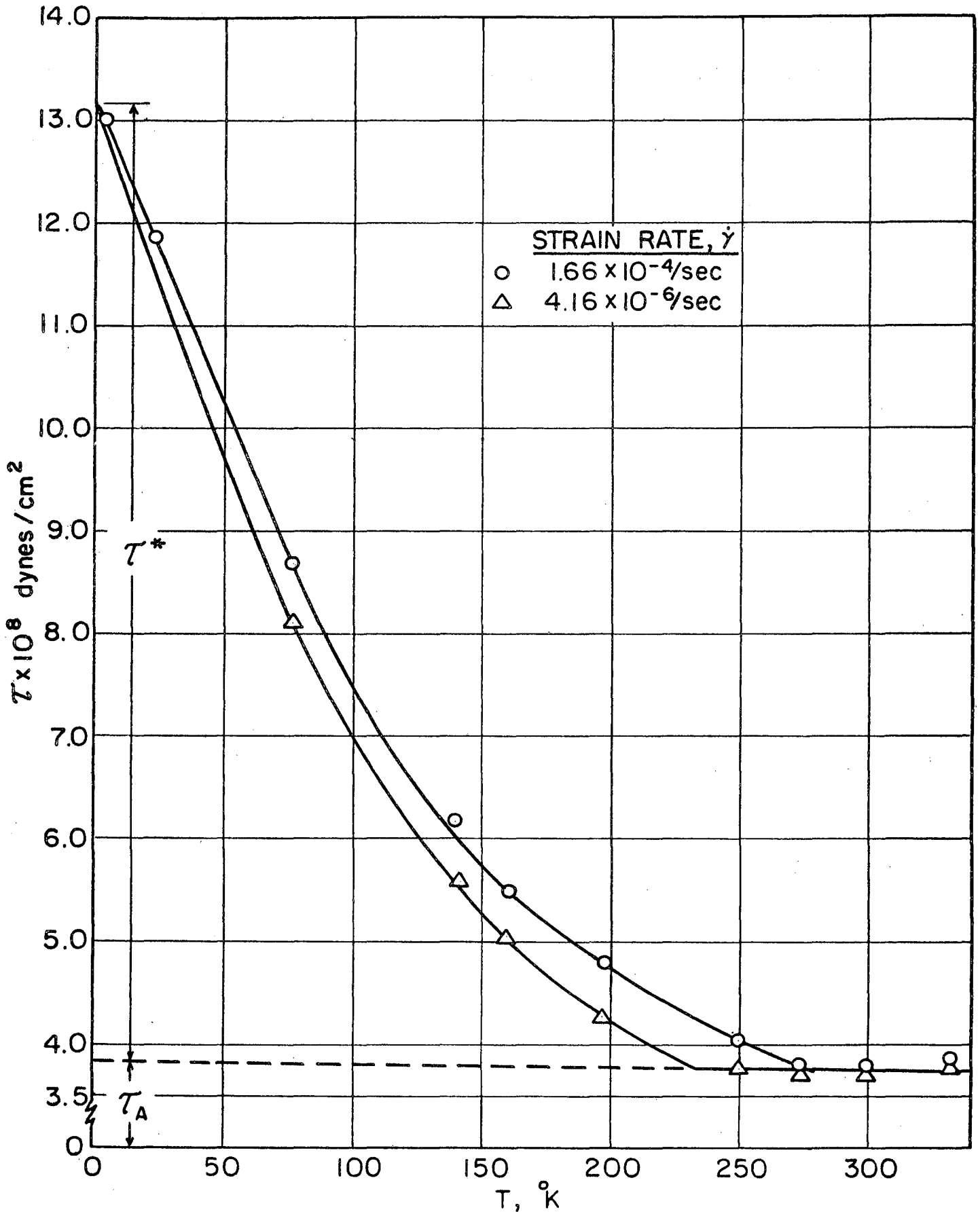


FIG. 1 CRITICAL RESOLVED SHEAR STRESS FOR FLOW, τ , vs. TEMPERATURE.

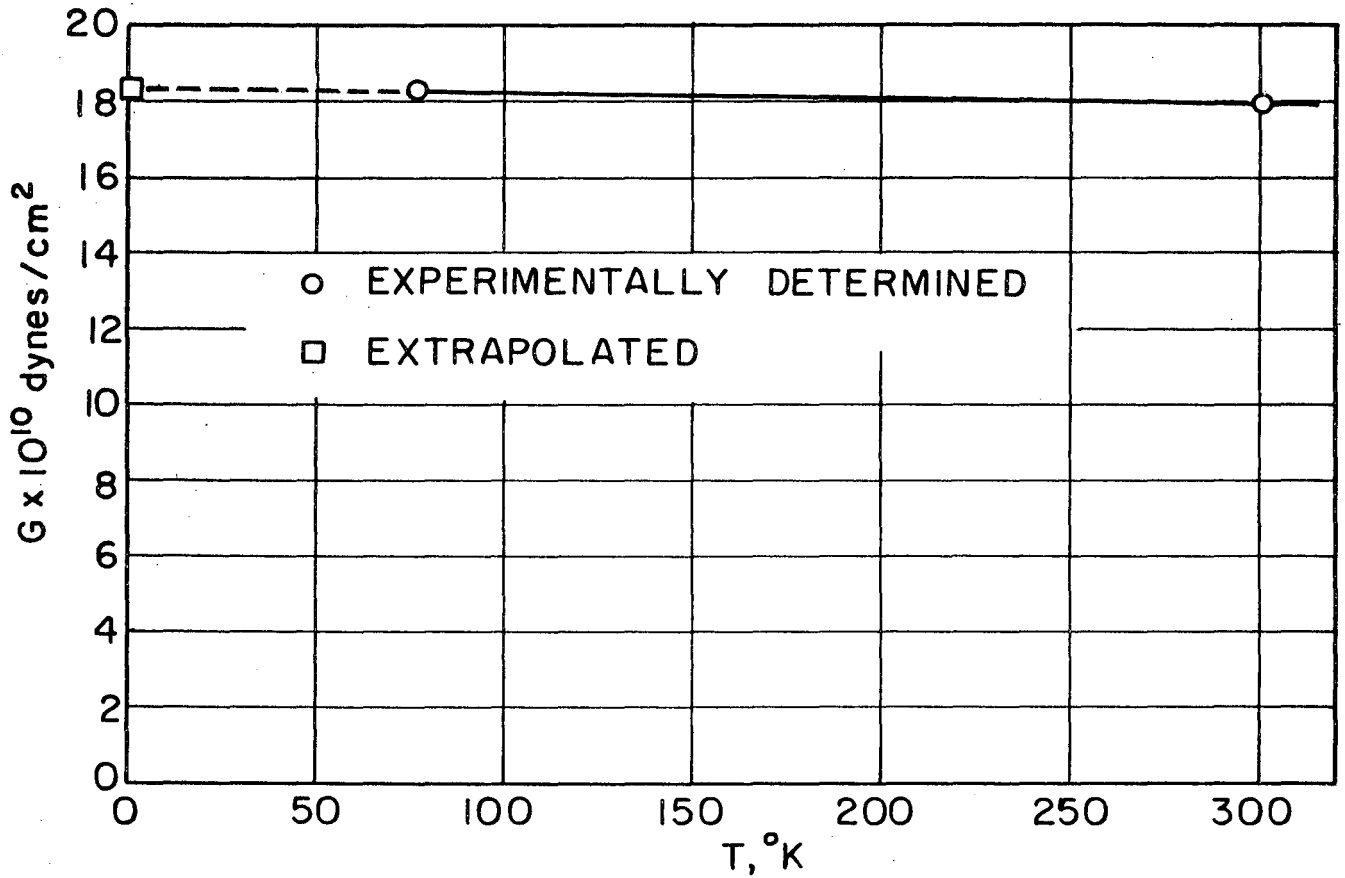


FIG. 2 VARIATION OF SHEAR MODULUS G IN $(\bar{3}21) [11]$ SYSTEM WITH TEMPERATURE.

The values of $\dot{\epsilon}_A^*$ which are now corrected for specimen variation in $\dot{\epsilon}_A$, are shown in Fig. 3 for two strain rates. It is obvious from Fig. 3 that there is a critical temperature, depending on the strain rate, where the thermally activated process changes into an athermal process. Let us call these temperatures T_{c_1} and T_{c_2} for the slower and faster strain rates respectively.

Instead of discussing individually the various mechanisms that might be rate-controlling, in this study, we will proceed to show how the experimental results can be correlated to the theoretical deductions of the recent approach to the Peierls mechanism when the deformation is controlled by the rate of nucleation of pairs of kinks, as put forward by Dorn and Rajnak.¹⁰ In their approach the activation energy of the Peierls process is the saddle-point activation energy for the nucleation of pairs of kinks, found as a function of the applied stress, the lattice constants, the height and shape of Peierls hill and the line energy of the dislocation. In Fig. 3, the shape of the $\dot{\epsilon}_A^*$ versus T curves agree well with those Dorn and Rajnak have predicted when plastic deformation arises from the nucleation of pairs of kinks. A significant feature of the nominal agreement between theory and experiment concerns the fact that both reveal that the $\dot{\epsilon}_A^*$ versus T curves have a finite slope as $\dot{\epsilon}_A^*$ approaches zero.

If a single mechanism is rate-controlling, the plastic strain rate $\dot{\gamma}$ is given by

$$\dot{\gamma} = \rho ab \frac{L}{\omega} \nu e^{-U_n/RT} \quad (3)$$

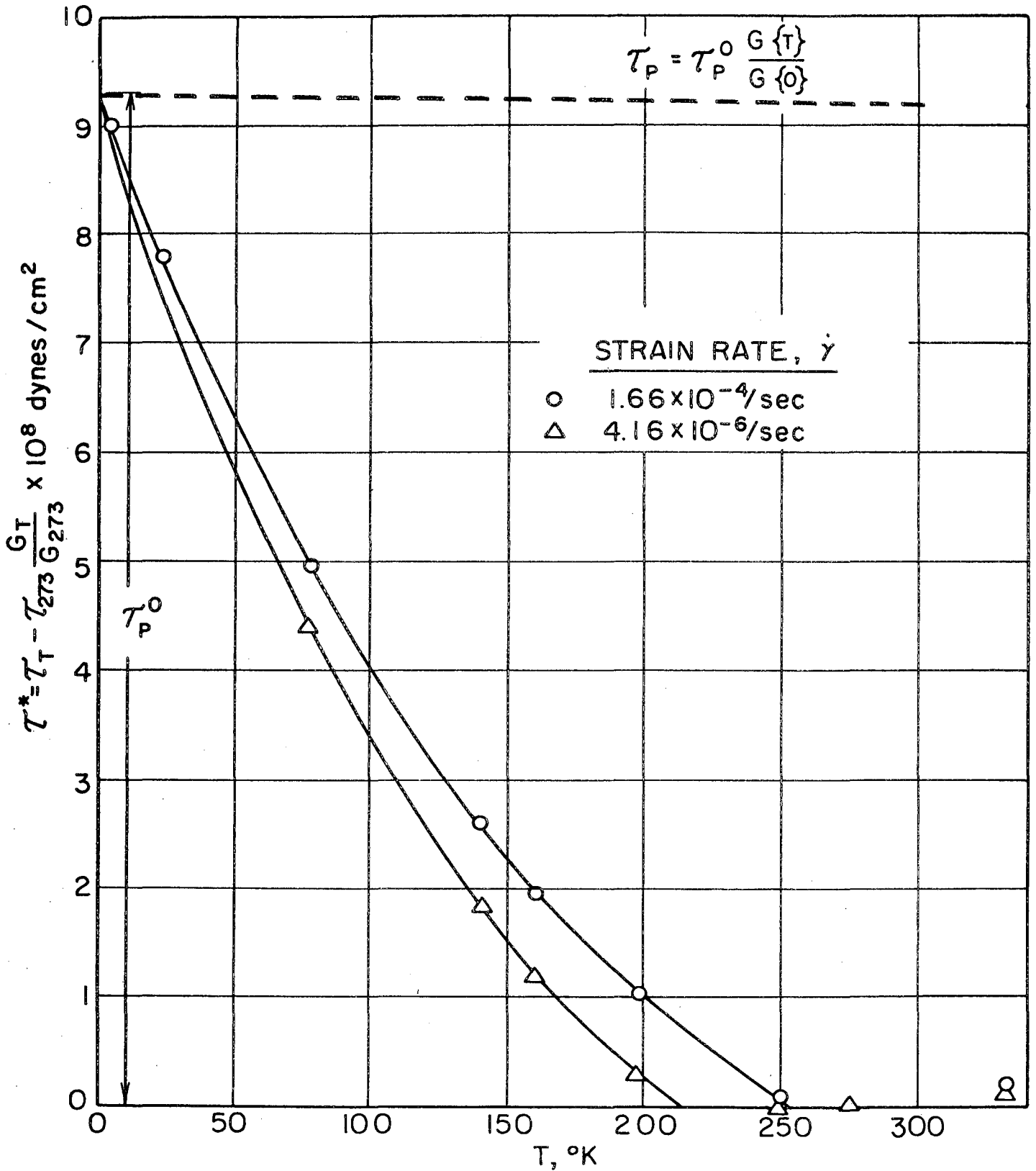


FIG. 3 THE THERMALLY ACTIVATED COMPONENT OF FLOW STRESS, τ^* , vs. TEMPERATURE.

where

ρ = density of mobile dislocations

a = the distance between Peierls valleys

b = Burgers vector

L = the mean, geometrically limited, length swept out by a pair of kinks once nucleation occurs in that length

ν = the Debye frequency

U_n = saddle-point free energy for nucleation of a pair of kinks

w = width of a pair of kinks at the saddle-point free energy configuration

k = Boltzmann constant

T = temperature in $^{\circ}\text{K}$

The theory gives $U_n/2U_k$ as a function of τ^*/τ_P where U_k is the kink energy and τ_P is the Peierls stress, as shown by the curves of Fig. 4, for each of a series of values of α , where α expresses the deviation of the shape of the Peierls hill from a sinusoidal periodic variation. The shape of the Peierls hill is defined in terms of α by

$$\Gamma_{\{y\}} = \left(\frac{\Gamma_c - \Gamma_0}{2} \right) + \left(\frac{\Gamma_c - \Gamma_0}{2} \right) \cos \frac{2\pi y}{a} + \alpha \left(\frac{\Gamma_c - \Gamma_0}{4} \right) \left(1 - \cos \frac{4\pi y}{a} \right) \quad (4)$$

where Γ_c is the line energy of a dislocation at the top of the Peierls hill, where $y = 0$, Γ_0 is the line energy in the valley where $y = \pm a/2$ and $\Gamma_{\{y\}}$ is the line energy when the dislocation is displaced a distance y from the top of the hill. At $T = T_c$ where τ^* first becomes zero, the thermal energy that need be supplied is just $U_n = 2U_k$, and therefore for this condition

$$\dot{\gamma} = \rho a b \nu \frac{L}{w_c} e^{-\frac{2U_k\{T_c\}}{RT_c}} \quad (5)$$

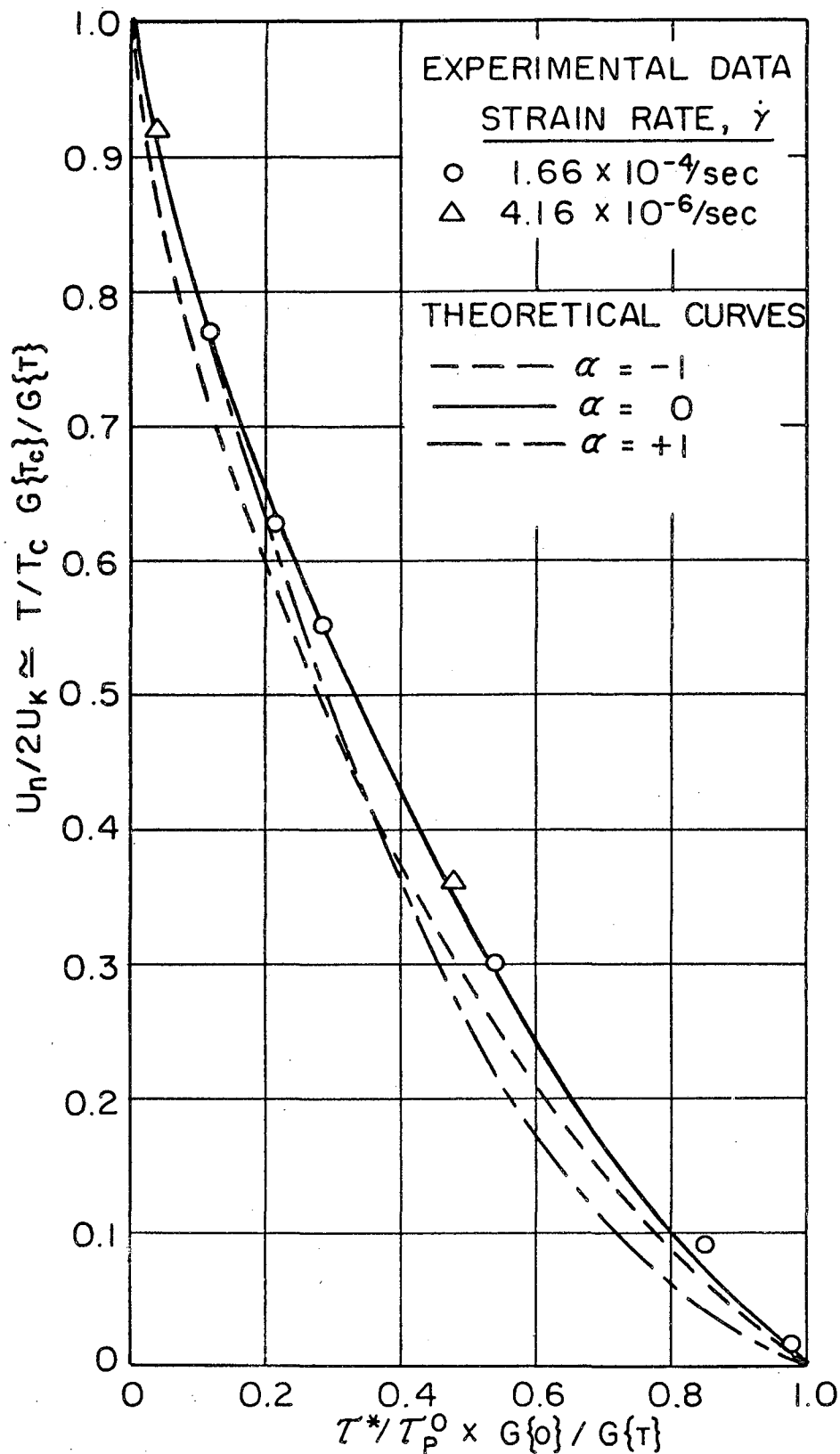


FIG. 4 THE THERMALLY ACTIVATED FLOW STRESS vs. TEMPERATURE IN DIMENSIONLESS UNITS.

But as shown by Dorn and Rajnak, to a very good approximation $w \simeq w_c$ and therefore from Eqns. 4 and 5

$$\frac{U_n\{T\}}{2U_k\{T\}} = \frac{U_n\{T\}}{2U_k\{T_c\}} \left(\frac{G\{T\}}{G\{T_c\}} \right) \simeq \frac{T}{T_c} \frac{G\{T_c\}}{G\{T\}} \quad (6)$$

Taking, furthermore, that the Peierls stress at the absolute zero is equal to \uparrow^* at the absolute zero, we obtain $\uparrow_P^0 = 9.25 \times 10^8 \text{ dynes/cm}^2$.

Although Kuhlmann-Wilsdorf¹¹ suggested that the Peierls stress decreased quite rapidly with an increase in temperature as a result of a "uncertainty concept", the justification for this assumption, as already pointed out by Friedel¹² is weak. The present work indicates that the Peierls stress decreased nearly linearly with an increase in temperature. We therefore assume that

$$\uparrow_P = \uparrow_P^0 \frac{G\{T\}}{G\{0\}} \quad (7)$$

as shown by the broken line on the top of Fig. 3. The experimental data $U_n/2U_k$ as a function of \uparrow^*/\uparrow_P as deduced with the aid of Eqns. 6 and 7 are shown by the points in Fig. 4. The expected theoretical trends as shown by the curves in Fig. 4 are in excellent agreement with the experimental data and it appears to agree best with the curve representing $\alpha = 0$, excluding the 23°K data where the temperature measurement is known to be somewhat in error.

Activation Energy for Nucleation of Pairs of Kinks

The activation energy can be determined if the change in strain rate due to change in temperature, at constant stress, is known. From Eqn. 5

$$\frac{\dot{\gamma}_2}{\dot{\gamma}_1} = \frac{e^{-\frac{2U_k\{0\}}{RT_{c_2}}}}{e^{-\frac{2U_k\{0\}}{RT_{c_1}}}} \frac{\frac{G\{T_{c_2}\}}{G\{0\}}}{\frac{G\{T_{c_1}\}}{G\{0\}}}$$

or

$$2U_k\{0\} = \frac{RG\{0\}}{\frac{G\{T_{c_1}\}}{T_{c_1}} - \frac{G\{T_{c_2}\}}{T_{c_2}}} \times \ln \frac{\dot{\gamma}_2}{\dot{\gamma}_1} \quad (8)$$

using

$$k = 1.38 \times 10^{-16} \text{ erg. per degree}$$

$$G\{0\} = 18.254 \times 10^{10} \text{ dynes/cm}^2$$

$$G\{T_{c_1}\} = 18.049 \times 10^{10} \text{ dynes/cm}^2$$

$$G\{T_{c_2}\} = 18.009 \times 10^{10} \text{ dynes/cm}^2$$

$$T_{c_1} = 214^\circ \text{K}$$

$$T_{c_2} = 256^\circ \text{K}$$

$$\ln \frac{\dot{\gamma}_2}{\dot{\gamma}_1} = \ln 40$$

$2U_{k_0}$ is equal to 0.664×10^{-12} erg. or to 0.41 ev., which is of the right order of magnitude for activation energy, when the rate-controlling mechanism is by nucleation of pairs of kinks.

Activation Volume

The most reliable verification of the Peierls process concerns agreement between theoretical and experimentally deduced activation volumes. The experimental activation volumes are obtained by the effect of small changes in strain rate on the flow stress. We define the quantity β as

$$\beta = \frac{\partial \ln \dot{\gamma}}{\partial \tau^*} = \frac{\partial \ln \rho}{\partial \tau^*} - \frac{\partial \ln \omega}{\partial \tau^*} - \frac{1}{RT} \frac{\partial U_n}{\partial \tau^*} \quad (9)$$

We take βRT as the apparent activation volume, v_a , where

$$v_a = \beta RT = RT \frac{\partial \ln \rho}{\partial \tau^*} - \frac{\partial \ln w}{\partial \tau^*} - \frac{\partial \ln \eta}{\partial \tau^*} \quad (10)$$

and the negative or last term of Eqn. 10 is the theoretical activation volume v^* . Whereas the term containing w is always negligibly small, v_a can on occasions be slightly larger than v^* , as a result of the possible increase in dislocation density, ρ , as the stress is increased. Figure 5 shows the v_a versus τ^* curve and the low values of v_a in terms of b^3 agree very well with the low activation volume as predicted for the Peierls process.

Figure 6 shows the theoretical plot for the activation volume versus τ^*/τ_P for different values of α . The experimental values of $-(\tau_P/2U_k) \frac{\partial \ln \eta}{\partial \tau}$ for different values of τ^*/τ_P^0 (corrected for change in shear modulus with temperature) are also plotted on the same figure. Again the correlations between experiment and theory are good and the data seems to be best fitted to the curve representing $\alpha = 0$.

Evaluation of Line Tension of Dislocation Situated at the Peierls Valley

Dorn and Rajnak gave the theoretical values of $\frac{\tau_{ab}}{\pi \tau_0}$ and $\frac{2U_k \pi}{\alpha \tau_0}$ for different values of α and $R - 1$, where $R = \tau_c/\tau_0$. In our case where $\alpha = 0$, using the experimentally determined values of τ_P and $2U_k$, one gets a pair of simultaneous equations involving R and τ_0 . Eliminating R , one gets the value of $\tau_0 = 2.284 \times 10^{-4}$ dynes.

Assuming $\tau_0 = \delta Gb^2$ and using $G = 18.03 \times 10^{10}$ dynes/cm² and $b = 5.724 \times 10^{-8}$ cm, δ is approximately equal to 0.4. Within the limits of experimental error, the experimental value of τ_0 is reasonable.

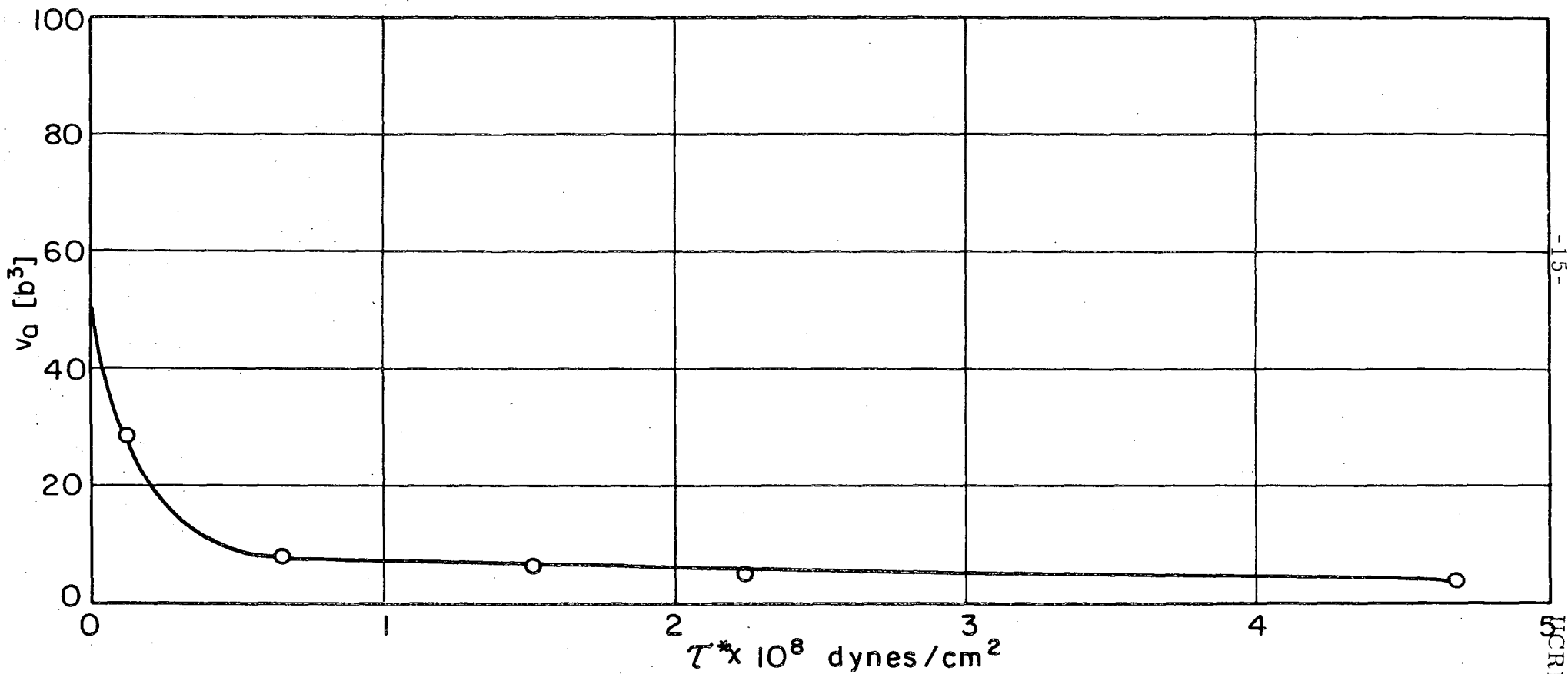


FIG. 5 APPARENT ACTIVATION VOLUME vs. THE THERMALLY ACTIVATED COMPONENT OF THE FLOW STRESS.

-15- UCRL-10916

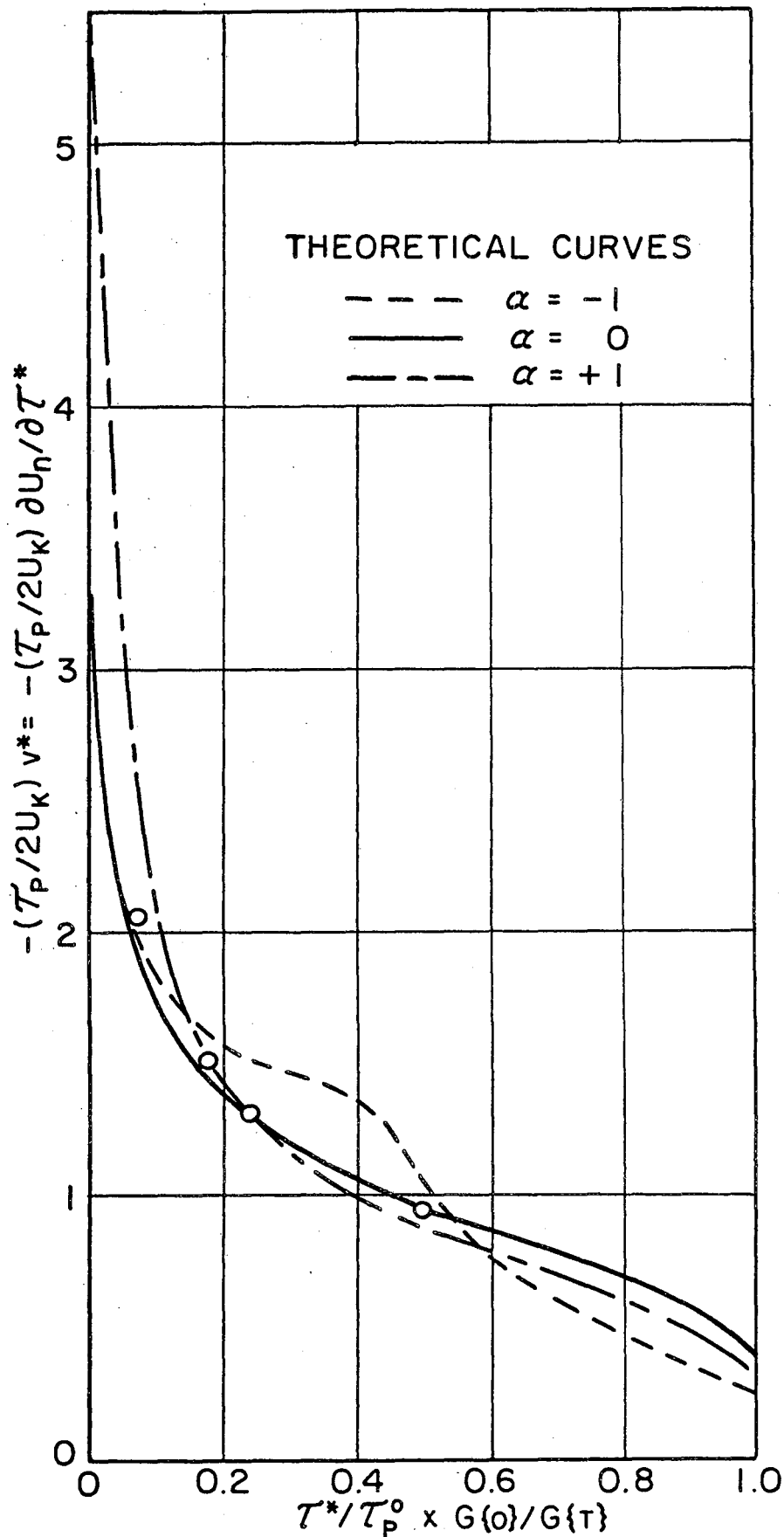


FIG. 6 THE THERMALLY ACTIVATED COMPONENT OF FLOW STRESS vs. ACTIVATION VOLUME IN DIMENSIONLESS UNITS. MU-31488

Experimental Values of ρL

For a given strain rate the value of ρL could be determined from Eqn. 5. Taking $50b$ for the value of w_c , and 6.52×10^{12} per second for the Debye frequency for AgMg and using the known values of $a, b, 2U_k, k$ and T_c , the value of ρL is equal to 227 per cm, which is of the right order of magnitude.

CONCLUSIONS

1. The deformation of single crystals of CsCl type of intermetallic compound AgMg has been investigated at the low temperature range, using two strain rates.

2. The relation of stress vs. temperature, activation energy vs. stress and activation volume vs. stress agree very well with the dictates of Peierls process when the rate-controlling mechanism is the nucleation of pairs of kinks.

3. The shape of the Peierls hill for AgMg approaches a purely sinusoidal variation with $\alpha = 0$.

4. The activation energy of the process of the nucleation of pairs of kinks is estimated to be 0.41 ev.

5. The apparent activation volume over the range where Peierls process is operative is approximately 3 to $8b^3$ at high stresses (4 to 13×10^8 dynes/cm²), approximately $30b^3$ at intermediate stresses (3 to 4×10^8 dynes/cm²), increasing to values of about $50b^3$ at lower stresses.

6. The experimentally deduced values of the dislocation line tension in the Peierls valley $\tau_0 = 2.28 \times 10^{-4}$ dynes and that of $\rho L = 227$ per cm. are within the right order of magnitude and could be said to be reasonable.

ACKNOWLEDGMENTS

This research was conducted as part of the activities of the Inorganic Materials Research Division of the Lawrence Radiation Laboratory of the University of California, Berkeley. The authors express their appreciation to the United States Atomic Energy Commission for their support of this effort. Thanks are also due to Mr. Robert Walson for the assistance he gave in growing the AgMg single crystals and to Mr. J. D. Mote for valuable suggestions in the experimental part of the program.

REFERENCES

1. J. H. Westbrook, ed., Mechanical Properties of Intermetallic Compounds, p. 1, John Wiley and Sons, Inc., 1960.
2. A. Westgren and G. Phragmen, *Metallwirtschaft* 7, 700-703 (1928).
3. W. L. Bragg and E. J. Williams, *Proc. Roy. Soc. (London)* A 151, 540 (1935).
4. J. H. Westbrook, *J. Electrochem. Soc.* 104, 369 (1957).
5. N. V. Ageev and V. G. Kuznetsov, *Bull. Acad. Sci. USSR*, 289 (1937).
6. W. J. Smirnov and N. S. Kurnakov, *Z. Anorg. Chem.* 72, 31 (1911).
7. W. A. Rachinger and A. H. Cottrell, *Acta Met.*, 4, 1 (1956).
8. D. L. Wood and J. H. Westbrook, *Trans. AIME* 224, 1024-1036 (1962).
9. A. Chang, "Variation of the Elastic Compliances of AgMg with Temperature" to be published.
10. John E. Dorn and Stanley Rajnak, "Nucleation of Kink Pairs and the Peierls' Mechanism of Plastic Deformation" submitted to *Trans. AIME*.
11. D. Kuhlmann-Wilsdorf, *Phys. Rev.* 120, 773 (1960).
12. J. Friedel, "On the Elastic Limit of Crystals" Electron Microscopy and Strength of Crystals, Interscience Pub., 605 (1963).

This report was prepared as an account of Government sponsored work. Neither the United States, nor the Commission, nor any person acting on behalf of the Commission:

- A. Makes any warranty or representation, expressed or implied, with respect to the accuracy, completeness, or usefulness of the information contained in this report, or that the use of any information, apparatus, method, or process disclosed in this report may not infringe privately owned rights; or
- B. Assumes any liabilities with respect to the use of, or for damages resulting from the use of any information, apparatus, method, or process disclosed in this report.

As used in the above, "person acting on behalf of the Commission" includes any employee or contractor of the Commission, or employee of such contractor, to the extent that such employee or contractor of the Commission, or employee of such contractor prepares, disseminates, or provides access to, any information pursuant to his employment or contract with the Commission, or his employment with such contractor.

